Cell PRESS
Open ACCESS

Cell Reports
Report

Convergent Evolution of Sodium Ion Selectivity in Metazoan Neuronal Signaling

Maya Gur Barzilai,[1] Adam M. Reitzel,[2] Johanna E.M. Kraus,[3] Dalia Gordon,[1] Ulrich Technau,[3] Michael Gurevitz,[1] and Yehu Moran[3,*]

[1]Department of Molecular Biology and Ecology of Plants, George S. Wise Faculty of Life Sciences, Tel-Aviv University, Tel-Aviv 69978, Israel
[2]Biology Department, Woods Hole Oceanographic Institution, Woods Hole, MA 02543, USA
[3]Department of Molecular Evolution and Development, Faculty of Life Sciences, University of Vienna, Althanstraße 14, 1090 Vienna, Austria
*Correspondence: yehu.moran@univie.ac.at
http://dx.doi.org/10.1016/j.celrep.2012.06.016

SUMMARY

Ion selectivity of metazoan voltage-gated Na^+ channels is critical for neuronal signaling and has long been attributed to a ring of four conserved amino acids that constitute the ion selectivity filter (SF) at the channel pore. Yet, in addition to channels with a preference for Ca^{2+} ions, the expression and characterization of Na^+ channel homologs from the sea anemone *Nematostella vectensis*, a member of the early-branching metazoan phylum Cnidaria, revealed a sodium-selective channel bearing a noncanonical SF. Mutagenesis and physiological assays suggest that pore elements additional to the SF determine the preference for Na^+ in this channel. Phylogenetic analysis assigns the *Nematostella* Na^+-selective channel to a channel group unique to Cnidaria, which diverged >540 million years ago from Ca^{2+}-conducting Na^+ channel homologs. The identification of Cnidarian Na^+-selective ion channels distinct from the channels of bilaterian animals indicates that selectivity for Na^+ in neuronal signaling emerged independently in these two animal lineages.

INTRODUCTION

The emergence of nervous systems that enable the integration of external stimuli and coordinated responses was a key event in the evolution of animal body plans. Signaling in these systems is based on fast and accurate propagation and conductance of action potentials involving voltage-gated sodium channels (Na_vs) (Hille, 2001; Meech and Mackie, 2007). Na_vs are membrane-spanning protein complexes that are composed of pore-forming α-subunits and auxiliary subunits, and conduct Na^+ ions in response to changes in the membrane potential (Catterall, 2000; Hille, 2001). The α-subunit, which belongs to a protein superfamily of voltage-gated Na^+, K^+, and Ca^{2+} channels (Na_vs, K_vs, and Ca_vs, respectively), consists of four domains (DI–DIV) arranged around a central ion-conducting pore. Each domain is comprised of six transmembrane segments (S1–S6), of which the positively charged S4 (voltage sensor) moves outward in response to membrane depolarization, leading to opening of the channel pore and ion conductance. Whereas the α-subunit of K_vs is a single domain tetramer, the α-subunits of Ca_vs and Na_vs are large monomers of four homologous, nonidentical domains (Hille, 2001).

Ion selectivity is crucial for fast and accurate signaling, and the emergence of Na^+-selectivity likely addressed a need to distinguish neuronal stimuli from intracellular signaling driven by Ca^{2+} (Hille, 2001; Meech and Mackie, 2007). The selectivity of Na_vs for Na^+ ions is attributed to the ion selectivity filter (SF), a ring of four amino acids (Asp, Glu, Lys, and Ala [DEKA]) that are contributed by the pore-lining loops (p-loop) of the four domains (Catterall, 2000). The Lys at the third position of the DEKA SF is critical for ion selectivity, as indicated by the increase in Ca^{2+} and K^+ conductance when it is substituted in mammalian Na_vs (Heinemann et al., 1992; Schlief et al., 1996). Although the DEKA SF is conserved in all vertebrate and many invertebrate Na_vs (Widmark et al., 2011), novel Na_v-like channels with a DEEA SF have been observed in many invertebrates, including arthropods, mollusks and tunicates (Zhou et al., 2004; Cui et al., 2012; Sato and Matsumoto, 1992; Nagahora et al., 2000). Still, only two of these Na_v-like channels, BSC1 of the cockroach *Blattella germanica* and DSC1 of *Drosophila melanogaster*, have been functionally expressed and shown to preferably conduct Ca^{2+} (Zhang et al., 2011; Zhou et al., 2004).

Understanding the evolutionary relationship between Na_v and Na_v-like channels may shed light on the development of ion selectivity, and requires a broad data set for phylogenetic analysis. Previous analyses either focused on vertebrate channels or mostly used fragmented and nonverified gene models from invertebrates (Goldin, 2002; Widmark et al., 2011; Liebeskind et al., 2011). These analyses showed that Na_v-like channels existed in the common ancestor of animals and their unicellular relatives, choanoflagellates, and are present in the apusozoan *Thecamonas trahens* (Liebeskind et al., 2011; Cai, 2012). Because apusozoans diverged before the fungal-metazoan split occurred (Derelle and Lang, 2012), Na_v-like channels emerged before nervous systems or multicellularity evolved. Because Na_v-like channels from early branching phyla of animals or their protist relatives have not been studied directly, their impact on the evolutionary history of neuronal signaling has remained unclear.

To address this critical gap in knowledge, we focused on obtaining a phylogenetic and functional characterization of Na_v-like channels from the phylum Cnidaria (sea anemones, corals,

hydroids, and jellyfish). This basal animal clade is a sister group to all higher animals (Bilateria) and was among the first lineages to develop a nervous system (Watanabe et al., 2009), and is therefore highly suitable for the study of Na_v evolution in animals.

RESULTS AND DISCUSSION

Characterization of Na_v-like Homologs from *N. vectensis*

To study cnidarian Na_v-like channels, we used the starlet sea anemone *Nematostella vectensis* (Cnidaria, Anthozoa), whose genome has been fully sequenced (Putnam et al., 2007). A homology search of the genome retrieved five putative Na_v genes. cDNA cloning and sequencing revealed SFs resembling those found in Na_v-like channels. Channels with DEKA SF are termed Na_v1; therefore, we named the Na_v-like channels Na_v2, and accordingly refer to the five *Nematostella* channels as $NvNa_v2.1$–2.5. To functionally characterize these channels, we expressed them in *Xenopus* oocytes and examined their ion selectivity.

$NvNa_v2.1$, bearing a DEEA SF, exhibited slowly developing activating and inactivating currents in response to depolarizing voltage pulses, and substantial tail currents when returned to a holding potential (Figure 1A). Such currents with a reversal potential (E_{rev}) of −13 ± 1.2 mV (n = 8; Figure S1A) are reminiscent of Cl^- ion conductance through Ca^{2+}-activated Cl^- channels endogenous to *Xenopus* oocytes (Barish, 1983). Because these currents were reduced by the Na_v1 blocker lidocaine, the Cl^- currents were apparently triggered by Ca^{2+} influx through $NvNa_v2.1$ (Figure S1B). We removed the Cl^- currents by injecting the Ca^{2+} chelator BAPTA into the oocytes, which uncovered voltage-dependent inward currents characterized by fast activation and slow inactivation kinetics, and E_{rev} = 21.6 ± 2.2 mV (n = 7; Figure S1C). Further, we eliminated the Ca^{2+}-induced Cl^- currents by injecting either BAPTA or EGTA, and substituted $CaCl_2$ in the ND96 bath solution with $BaCl_2$, which is less likely to activate Ca^{2+}-activated Cl^- channels (Barish, 1983). Under these conditions, the inward currents measured were similar to those obtained with $CaCl_2$ (E_{rev} = 16.2 ± 0.8 mV, n = 14; Figures 1B and 1D). Whereas 100 μM tetrodotoxin (TTX), a Na_v1 blocker, had no effect (Figure S1D), lidocaine inhibited these currents in a dose-dependent manner (Figure 1E), suggesting a structural similarity between Na_v2 and Na_v1 channels at the lidocaine-binding site (Cestèle and Catterall, 2000). Moreover, in the presence of >10 mM lidocaine in the medium, *N. vectensis* adult polyps were paralyzed within 20 min. The lidocaine effects observed in vitro and in vivo suggest that the Na_v2 channels in *N. vectensis* have a crucial physiological role.

We next examined the $NvNa_v2.1$ ion conductance by substituting Na^+ in the bath solution with impermeable choline ions. Because the reversal potentials with and without Na^+ in the bath solution were similar (E_{rev} Na^+ = 16.2 ± 0.8 mV, n = 14; E_{rev} choline = 13.3 ± 0.9 mV, n = 12; Figures 1C and 1D), Ba^{2+} ions were evidently responsible for most of the current measured, implying that under physiological conditions, Ca^{2+} ions are the main charge carrier conducted by these channels. Using single ion solutions of identical concentrations, we found that the channel was also permeable to Na^+ and K^+ ions (permeability ratio P_K/P_{Na} = 1; Figure 2A).

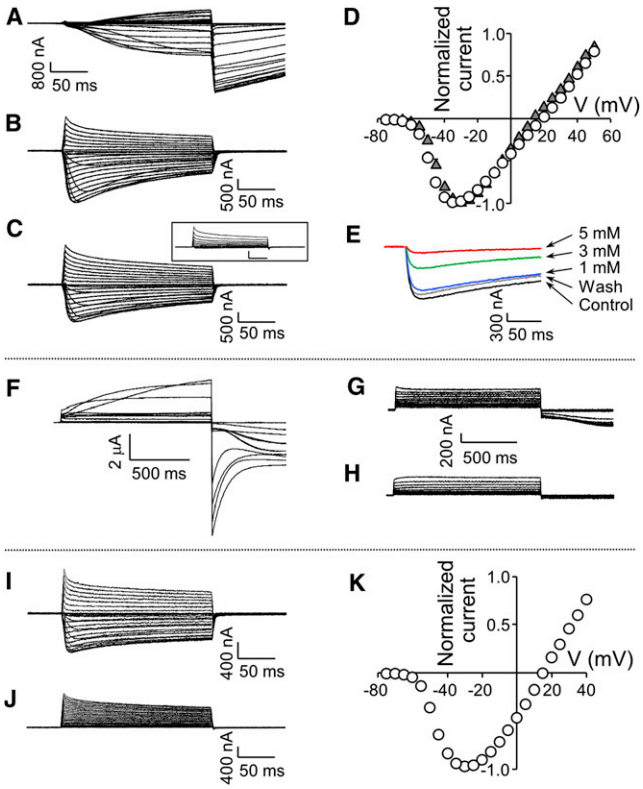

Figure 1. Current Recordings from $NvNa_v2.1$, $NvNa_v2.2$, and $NvNa_v2.1^{DEKA}$ Channels Expressed in *Xenopus* Oocytes

Oocytes were clamped at −80 mV holding potential, and currents were elicited by 200 ms depolarizations from −75 mV to 50 mV.

(A) Ca^{2+}-activated Cl^- currents recorded in ND96 bath solution from an oocyte expressing $NvNa_v2.1$.

(B–E) $NvNa_v2.1$ currents recorded in bath solution with Ba^{2+} substituting for Ca^{2+}, and in addition with choline substituting for Na^+ (C) and also without Ba^{2+} as control (see inset). See Figure S1 for further characterization of $NvNa_v2.1$.

(D) Current-voltage relations of $NvNa_v2.1$ (circles: E_{rev} = 16.2 ± 0.8 mV; n = 14) and with choline substituting for Na^+ (triangles: E_{rev} = 13.3 ± 0.9 mV; n = 7).

(E) Inward currents elicited by 200 ms depolarizing pulse to −30 mV in the presence of increasing concentrations of lidocaine. The inhibitory effect of lidocaine was removable by washes with bath solution (gray).

(F) Outward and tail currents elicited by 1 s depolarizations from −75 mV to 50 mV, measured for an oocyte expressing $NvNa_v2.2$ in ND96 bath solution.

(G and H) Currents decreased in the presence of 5 mM lidocaine (G) and were eliminated when Ca^{2+} was substituted with Ba^{2+} ions in the bath solution (H).

(I and J) $NvNa_v2.1^{DEKA}$ currents in ND96 bath solution (I) and with choline substituting for Na^+ (J).

(K) Current-voltage relations of $NvNa_v2.1^{DEKA}$ in ND96 bath solution (E_{rev} = 16.7 ± 1.1 mV; n = 14). Each point represents the mean ± SEM of n cells.

See also Figure S1.

In contrast to $NvNa_v2.1$, $NvNa_v2.2$, bearing a DEET SF, did not exhibit inward currents under various voltage protocols, but lidocaine-sensitive outward and tail currents in ND96 bath solution (with $CaCl_2$) were observed (Figures 1F and 1G). Because no inward currents were detected with Ba^{2+} substitution for Ca^{2+} (Figure 1H), the tail currents observed were of Ca^{2+}-activated Cl^- channels, indicating that $NvNa_v2.2$ conducts Ca^{2+} ions.

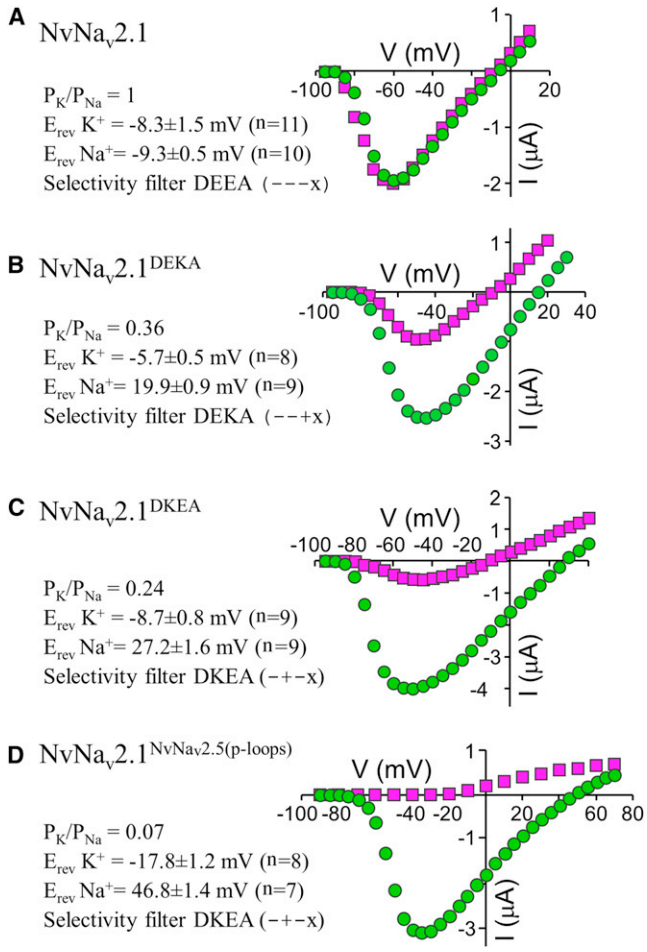

Figure 2. Current-Voltage Relations for NvNa$_v$2.1 Mutants in Na^+ and K^+ Single Ion Solutions and Relative Permeabilities

Currents were elicited for 200 ms from −95 up to 70 mV from a holding potential of −100 mV.

(A–D) Current-voltage relations of representative oocytes expressing NvNa$_v$2.1 (A), NvNa$_v$2.1^{DEKA} (B), NvNa$_v$2.1^{DKEA} (C), or NvNa$_v$2.1$^{NvNav2.5(p-loops)}$ (D). Circles: Na^+ single ion solution; squares: K^+ single ion solution. The relative ion permeability was calculated from the difference in reversal potential between K^+ and Na^+ single ion solutions of identical concentrations (see Experimental Procedures). The values provided are the mean ± SEM of n cells. The protonation state of each SF residue is indicated in parentheses, with x designating an uncharged residue.

See also Figure S2.

We further examined the ion selectivity by introducing the DEKA SF, which is conserved in all Na$_v$1 channels, in the background of NvNa$_v$2.1 (substitution E1239K, mutant NvNa$_v$2.1^{DEKA}). No inward current was detectable when Na^+ in the bath solution was substituted with choline, indicating that the channel mutant was Ca^{2+} impermeable (E_{rev} = 16.7 ± 1.1 mV, n = 14; Figures 1I–1K). However, whereas Na$_v$1 channels are Na^+ selective ($P_K/P_{Na} \leq 0.1$; Schlief et al., 1996), NvNa$_v$2.1^{DEKA} conducted both Na^+ and K^+ ions (P_K/P_{Na} = 0.36; Figure 2B). This finding substantiates the structural difference between Na$_v$1 and Na$_v$2 at the channel pore.

NvNa$_v$2.5 Is a Na^+-Selective Channel

The unique DKEA SF (Figure 3A) raised questions regarding the ion preference of NvNa$_v$2.5. Because NvNa$_v$2.5 did not express in oocytes, we used NvNa$_v$2.1 as a platform for analysis of NvNa$_v$2.5 ion selectivity. Substitution E800K at DII resulted in mutant NvNa$_v$2.1^{DKEA}, which exhibited biphasic inward currents with a first peak that appeared within milliseconds and a second, slowly developing peak with tail currents (Figure 3B). Substituting Na^+ with choline or chelating the Ca^+ in the bath solution with EGTA (Figures 3C and 3D) indicated that the first peak corresponded to Na^+ currents and the second peak corresponded to Cl^- currents induced by Ca^{2+} conducted by NvNa$_v$2.1^{DKEA}. Furthermore, inward currents were observed in K^+ single ion solution, indicating that NvNa$_v$2.1^{DKEA} is nonselective (P_K/P_{Na} = 0.24; Figure 2C). However, in comparison with NvNa$_v$2.1, which conducts mainly Ca^{2+}, considerable Na^+ currents were measured through NvNa$_v$2.1^{DKEA}.

The p-loops of NvNa$_v$2.5 differ in sequence from those of the other four NvNa$_v$2 channels (Figure 3A). Moreover, transcripts encoding Na$_v$2.5 homologs with DKEA SF were previously identified in motor neurons of the hydrozoan *Polyorchis penicillatus* and the scyphozoan *Cyanea capillata*, and whole-cell recording in *P. penicillatus* showed Na^+-selective voltage-gated ion currents (Anderson et al., 1993; Spafford et al., 1996). Therefore, we constructed the NvNa$_v$2.5 p-loops of all four domains in the background of NvNa$_v$2.1 and examined the ion selectivity. The resulting channel chimera, NvNa$_v$2.1$^{NvNav2.5(p-loops)}$, was Ca^{2+} impermeable (Figures 3E and 3F), with an E_{rev} value of 46.5 ± 1.2 mV (n = 19; Figure 3G) and P_K/P_{Na} ratio of 0.07 (Figure 2D) resembling those of Na$_v$1 channels (insect channel DmNa$_v$1 E_{rev} = 47.8 ± 1.1 mV, n = 17; mammalian brain channel rNa$_v$1.2 E_{rev} = 48.9 ± 2.3 mV, n = 14; data not shown). These characteristics suggest that NvNa$_v$2.1$^{NvNav2.5(p-loops)}$ is Na^+ selective. Of note, the Na^+ selectivity was lost when the DKEA SF was substituted with DEEA or DEKA (Figure S2).

Based on mutagenesis of the Na$_v$1 DEKA SF, DKEA in the Na$_v$2.5 channel was considered an intermediate between DEKA and DEEA SFs (Schlief et al., 1996; Liebeskind et al., 2011). However, here we show not only that NvNa$_v$2.5 is as Na^+ selective as Na$_v$1, but also that this selectivity cannot be conferred by the DKEA SF alone. Because Na^+ selectivity in NvNa$_v$2.1 was achieved only when the entire p-loop region was exchanged by that of NvNa$_v$2.5, other residues in addition to those of the SF are involved in determining the Na^+ selectivity of NvNa$_v$2.5.

The multiple Na$_v$2 genes in *N. vectensis* suggested variable spatiotemporal expression, and indeed this was demonstrated by quantitative PCR (qPCR) analysis and distinct in situ hybridization expression patterns (Figure S3). Using two *Clytia hemisphaerica* sodium channel cDNA clones homologous to NvNa$_v$2.1 and NvNa$_v$2.5 (ChNa$_v$2.1 and ChNa$_v$2.5), and in situ hybridization, we observed differential channel expression in two distinct developmental stages of this hydrozoan (Figures S3G–S3J). Thus, similarly to bilaterian animals, cnidarians possess several channel subtypes distributed in a spatiotemporal manner, possibly reflecting specialized physiological

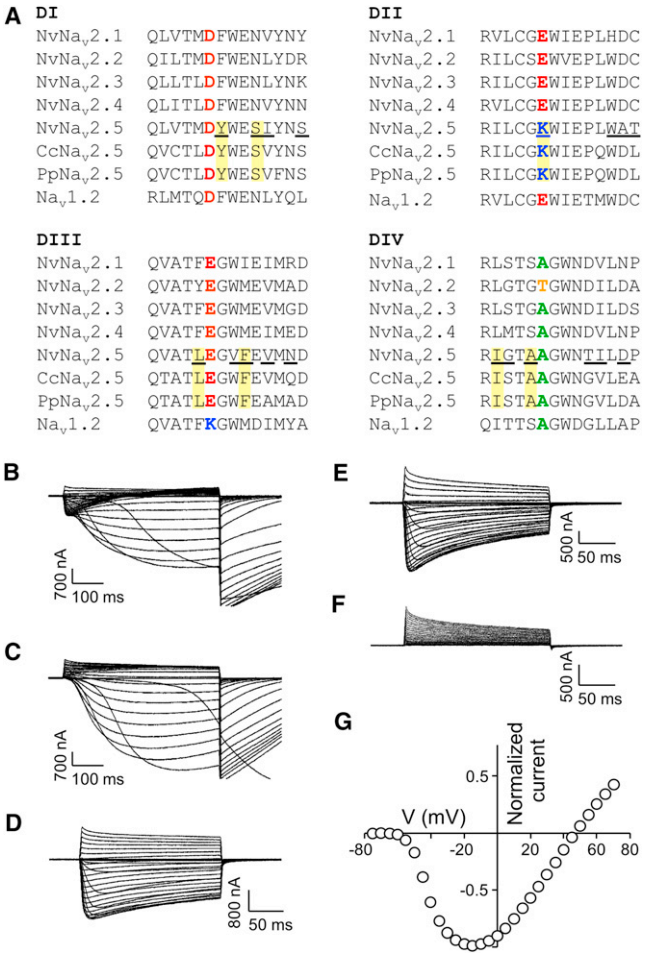

Figure 3. Sequence Alignment of $NvNa_v2$ Channels and Current Recordings from $NvNa_v2.1^{DKEA}$ and $NvNa_v2.1^{NvNav2.5(p-loops)}$ Channels Expressed in *Xenopus* Oocytes

(A) Alignment of the pore-loop regions of the five *N. vectensis* (Nv) channels (see also Figure S3 for spatiotemporal expression of Na_v2 cnidarian channels), as well as a channel from the medusae *P. penicillatus* (Pp) and *C. capillata* (Cc) and the mammalian brain channel $Na_v1.2$. Substitutions of $NvNa_v2.1^{NvNav2.5(p-loops)}$ are underlined and substitutions unique to the $Na_v2.5$ channel subfamily are in yellow boxes. For current recordings the oocytes were clamped at −80 mV holding potential and currents were elicited by 200 or 500 ms depolarizing voltage pulses from −75 mV to either 50 or 70 mV.

(B) $NvNa_v2.1^{DKEA}$ in ND96 bath solution.

(C) $NvNa_v2.1^{DKEA}$ with choline substituting for Na^+ in the bath solution.

(D) $NvNa_v2.1^{DKEA}$ with Ca^{2+} in the bath solution chelated by EGTA.

(E and F) $NvNa_v2.1^{NvNav2.5(p-loops)}$ in ND96 bath solution (E) and with choline substituting for Na^+ (F).

(G) Current-voltage relations of $NvNa_v2.1^{NvNav2.5(p-loops)}$ (E_{rev} = 46.5 ± 1.2 mV; n = 19). Each point represents mean ± SEM of n cells (see Figure S2 for analysis of the SF in $NvNa_v2.1^{NvNav2.5(p-loops)}$).

roles. Given the complex expression of other neuronal genes in *N. vectensis* (Marlow et al., 2009) and the correlation between the increase in the number of Na_v genes and neuronal complexity in bilaterians (Widmark et al., 2011), cnidarian excitability is probably more complex than was initially hypothesized.

Na^+-Channel Phylogeny Reveals Convergent Evolution of Sodium Selectivity

The characterization of sea anemone Na_v2 channels, especially the Na^+-selective $NvNa_v2.5$, prompted us to reanalyze the evolutionary history of sodium channels. We extended the data set of Na_v sequences with full-length cDNAs encoding Na_v2 homologs, which we cloned from basal metazoans and their relatives (Figure 4 and Table S1). We also identified and cloned $Na_v2.1$ and $Na_v2.5$ homologs from the hydroid cnidarians *Hydra magnipapillata* (Chapman et al., 2010) and *Clytia hemisphaerica* (J.E.M.K., unpublished data). Our phylogenetic analysis with the extended data set using the putative channel of the diatom *Thalassiosira pseudonana* as an outgroup (Derelle and Lang, 2012) positioned the Na_v2 channels within a single cluster containing all metazoan Na_vs and a putative homolog from *T. trahens* (Figure 4). This phylogeny confirms that Na_v2 channels appeared prior to the metazoan-fungal split (Cai, 2012), and that they were retained in most extant nonbilaterian animals but not in fungi or the unicellular opisthokont *Capsaspora owczarzaki*. Na_v2 channels are also found in many bilaterians, but were lost in vertebrates. Na_v1 channels, however, are found only in bilaterians (Figure 4; Liebeskind et al., 2011). Although Na_v2 channels mediate Ca^{2+}, they cluster with Na_v1 channels rather than Ca_vs. Because Na_v2 channels coexisted with Ca_vs in the ancestor of *T. trahens* and opisthokonts (Cai, 2012), the separation of Na_vs from Ca_vs occurred more than a billion years ago.

The *N. vectensis* channels ($NvNa_v2.1$–$NvNa_v2.5$) are clustered with channels of other cnidarians, indicating a monophyletic origin (Figure 4). $NvNa_v2.5$, however, forms a small subcluster together with hydrozoan and scyphozoan Na_vs bearing a unique DKEA SF, suggesting that the $Na_v2.1$ and $Na_v2.5$ subtypes resulted from a gene duplication event in the common ancestor of all extant cnidarians >540 million years ago (Park et al., 2012). The selective Na^+ conductance of the $Na_v2.5$ subfamily explains the sodium-based action potentials measured in isolated motor neurons of the medusozoans *Cyanea* and *Polyorchis* (Anderson, 1987; Spafford et al., 1996).

Our results indicate that selectivity for Na^+ evolved separately in the cnidarian and bilaterian lineages. Moreover, a single substitution at the third position in the SF of $NvNa_v2.1$, to resemble the DEKA SF of Na_v1 channels ($NvNa_v2.1^{DEKA}$), abolished Ca^{2+} but not K^+ conductance. Because K^+ ion conductance through K_vs generates the falling phase of the action potential, whereas Na^+ ion conductance through Na_vs is responsible for its rising phase, a clear functional advantage would be gained by separating these two fluxes and increasing the selectivity of Na_v2 channels to Na^+ ions. We therefore propose that the pore regions in both the urbilaterian Na_v1 and the primordial $Na_v2.5$ cnidarian channel evolved under selective pressure to cease K^+ and Ca^{2+} ion conductance, and that this required additional substitutions at the p-loops other than those at the SF. The selectivity for Na^+ was achieved in the two channel types in different ways, as is evident from the lack of selectivity for Na^+ ions in channel mutants $NvNa_v2.1^{NvNav2.5(p-loops\ DEKA)}$ bearing the SF of Na_v1, and $Na_v1.2^{DKEA}$ (a mammalian brain channel mutant) bearing the SF of $NvNa_v2.5$ (Figure S2; Schlief et al., 1996). This conclusion argues for a structural difference between the pore regions of $Na_v2.5$ and Na_v1, which is conceivable given

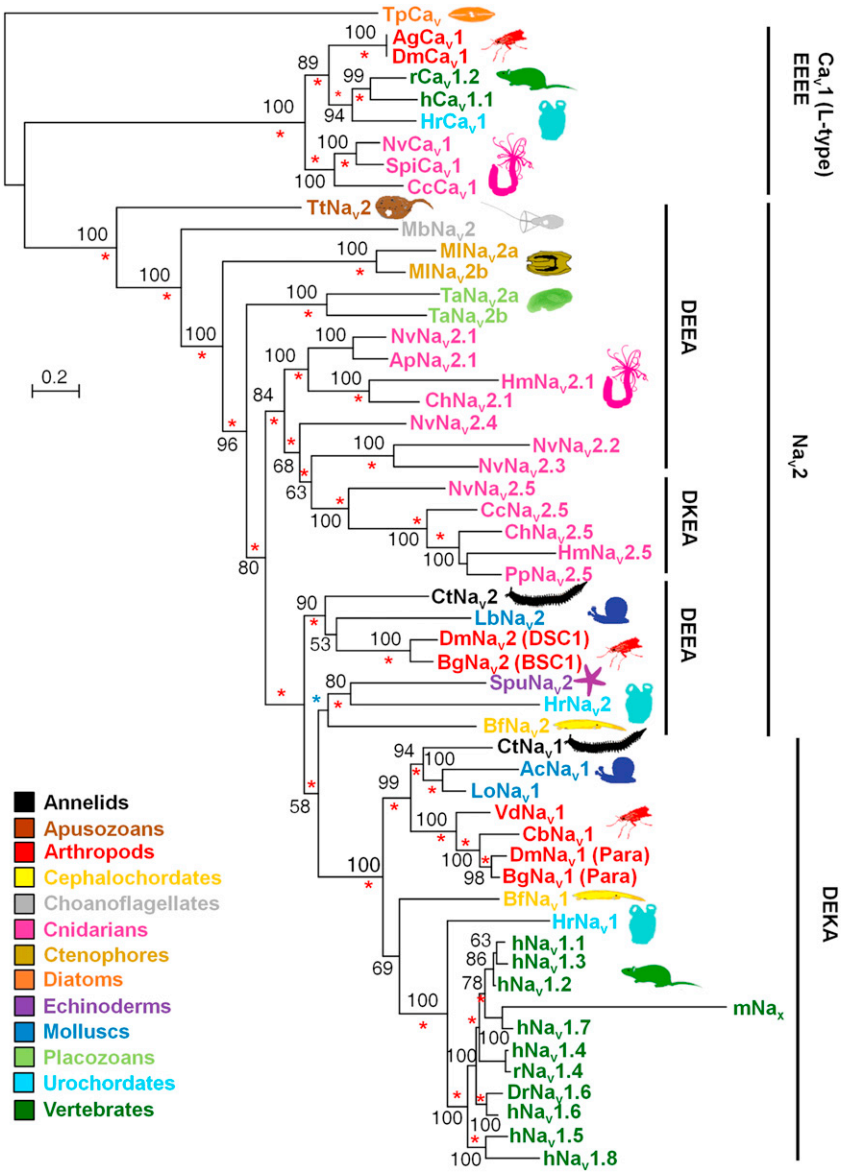

Figure 4. Phylogeny of Voltage-Gated Sodium Channels

A maximum-likelihood tree was constructed using the LG (+F +G +I) model. The bootstrap support out of 100 is indicated at the branches. A Bayesian analysis using the WAG model resulted in identical topology. Posterior probabilities of 1.0 are indicated by a red asterisk, and those of $0.95 < X < 1.0$ are indicated by a blue asterisk. All sequences are from cloned cDNA unless otherwise mentioned. Accession numbers and species names are available in Table S1. Animal clades are indicated by colors.

that Na^+ selectivity in cnidarian $Na_v2.5$ channels and bilaterian Na_v1 channels has evolved in a convergent manner.

Bacterial homotetrameric Na_vs bear an EEEE SF similar to that of metazoan Ca_vs, but they are still selective for Na^+ ions (Payandeh et al., 2011). Thus, Na^+ selectivity in voltage-gated ion channels evolved independently in three lineages on the tree of life. This highlights the plasticity of molecular evolution and the importance of Na^+ selectivity in biological systems ranging from prokaryotes to advanced eukaryotes.

Intriguingly, despite the advantages of Na^+ selectivity, several animal lineages with simple nervous systems (e.g., nematodes and echinoderms) appear to have independently lost the Na_v1 channels (Figure 4; Widmark et al., 2011; Jegla et al., 2009). Moreover, Na_v2 channels with a Ca^{2+} preference were retained in parallel to Na^+ selective channels in many animal groups, such as ascidians, insects, and cnidarians (Figure 4; Nagahora et al., 2000; Cui et al., 2012). Thus, it seems that Ca^{2+}-based action potentials are not merely an evolutionary relic but may be advantageous in simple neuronal circuits.

EXPERIMENTAL PROCEDURES

Identification of Na_v Homologs

Putative Na_v homologs were detected in GenBank (nr), Broad Institute, and Joint Genome Institute databases via BLAST. The voltage sensors, SF, and inactivation loop were assigned manually. Because some of these regions were missing or contained noncanonical substitutions, we cloned and sequenced overlapping cDNA fragments encoding the putative Na_vs from several basal metazoans and a choanoflagellate (see Table S1).

Functional Expression of Na_vs in Oocytes and Two-Electrode Voltage Clamp Measurements

Na_v-like transcripts were cloned into a modified pAlter expression vector (Promega). Constructs encoding the Na_v α-subunits were linearized, transcribed in vitro, and injected into *Xenopus* oocytes as described previously (Shichor et al., 2002). Currents were measured 1–3 days later using a two-electrode voltage clamp and a Gene Clamp 500 amplifier (Axon Instruments). Data were sampled at 10 kHz and filtered at 5 kHz. Unless otherwise stated, the ND96 bath solution contained (in mM) 96 NaCl, 2 KCl, 1 $MgCl_2$, 1.8 $CaCl_2$, 5 HEPES, pH 7.5. For G-V analysis, the mean conductance (G) was calculated from the peak current-voltage relations using the equation $G = I/(V - E_{rev})$, where I is the peak current, V is the membrane potential, and E_{rev} is the reversal potential. The normalized conductance-voltage relations were fit with either a one- or two-component Boltzmann distribution according to the equation:

$$\frac{G}{G_{max}} = \frac{(1-A)}{(1+\exp[(V1_{1/2}-V)/k_1])} + \frac{A}{(1+\exp[(V2_{1/2}-V)/k_2])},$$

where $V1_{1/2}$ and $V2_{1/2}$ are the respective membrane potentials for two populations of channels for which the mean conductance is half maximal, k_1 and k_2 are their respective slopes, and A defines the proportion of the second population (amplitude) over the total. When only one population of channels was apparent, A was set to zero. To avoid the Ca^{2+}-activated chloride currents in oocytes expressing $NvNa_v2.1$, $CaCl_2$ in the ND96 bath solution was substituted with $BaCl_2$, and the oocytes were injected 30 min or 2 hr prior to

the measurements with 25 nL of either 50 mM BAPTA or EGTA, respectively. The relative ion permeability P_K/P_{Na} was determined by measuring the difference in reversal potential between the test solution (K^+ single ion solution) and the reference solution (Na^+ single ion solution; see Extended Experimental Procedures). In the case of equal concentrations, the following equation was used (Hille, 2001):

$$\Delta E_{rev} = E_{rev}(X) - E_{rev}(Na) = \frac{RT}{F} \ln\left(\frac{P_X}{P_{Na}}\right),$$

where R, T, and F are the gas constant, absolute temperature, and Faraday's constant, respectively.

Characterization of Spatiotemporal Expression Patterns

The main parameters of the qPCR analysis followed an established protocol (Reitzel and Tarrant, 2009; see Extended Experimental Procedures). In situ hybridization in *N. vectensis* was carried out according to an established method (Genikhovich and Technau, 2009). *C. hemisphaerica* young medusae and gastrozoids were fixed in 3.7% formaldehyde and 0.2% glutaraldehyde in seawater for 1 hr at 4°C. In situ hybridization in *Clytia* was performed according to the *N. vectensis* protocol, but specimens were digested in a higher concentration of Proteinase K (0.02 mg/ml) to improve permeability.

Phylogenetic Analysis

Channel protein sequences were aligned with the use of MUSCLE (Edgar, 2004), and low-quality alignment regions were removed by the TrimAl program (Capella-Gutiérrez et al., 2009). ProtTest was used to determine the most suitable model for phylogenetic reconstruction of Na_Vs (Abascal et al., 2005). A maximum-likelihood phylogenetic tree was constructed using PhyML with the LG Model (+I +G +F; Guindon et al., 2010). Support values were calculated using 100 bootstrap replicates. Bayesian phylogenetic reconstruction was carried out using MrBayes 3.1 and the WAG model. A total of 5,000,000 generations were calculated and every 100th generation was sampled.

ACCESSION NUMBERS

All novel sequences have been deposited in GenBank under accession numbers HQ877452–HQ877461 and JQ066819–JQ066822.

SUPPLEMENTAL INFORMATION

Supplemental Information includes Extended Experimental Procedures, three figures, and one table and can be found with this article online at http://dx.doi.org/10.1016/j.celrep.2012.06.016.

LICENSING INFORMATION

ACKNOWLEDGMENTS

We thank N. King and M.J. Westbrook (University of California, Berkeley), L.Z. Holland (University of California, San Diego), P.A.V. Anderson (University of Florida), and B. Schierwater and M. Eitel (Institut für Tierökologie und Zellbiologie, Hannover) for providing RNA and tissue samples; D. Fredman (University of Vienna) for sharing data; and T.J. Jegla (Penn State University) and N. Dascal (Tel Aviv University) for critical comments. Y.M. was supported by an EMBO long-term fellowship (ALTF 1096-2009). A.M.R. was supported by award F32HD062178 from the Eunice Kennedy Shriver National Institute of Child Health and Human Development. This study was supported by a research grant from the Austrian National Science Foundation (FWF P 21108-B17) to U.T., and by a United States-Israel Binational Agricultural Research and Development Grant (IS-4313-10) and an Israeli Science Foundation grant (107/08) to M.G.

Received: February 20, 2012
Revised: May 14, 2012
Accepted: June 21, 2012
Published online: July 26, 2012

REFERENCES

Abascal, F., Zardoya, R., and Posada, D. (2005). ProtTest: selection of best-fit models of protein evolution. Bioinformatics *21*, 2104–2105.

Anderson, P. (1987). Properties and pharmacology of a TTX insensitive Na^+ current in neurones of the jellyfish *Cyanea Capillata*. J. Exp. Biol. *133*, 231–248.

Anderson, P.A., Holman, M.A., and Greenberg, R.M. (1993). Deduced amino acid sequence of a putative sodium channel from the scyphozoan jellyfish *Cyanea capillata*. Proc. Natl. Acad. Sci. USA *90*, 7419–7423.

Barish, M.E. (1983). A transient calcium-dependent chloride current in the immature *Xenopus* oocyte. J. Physiol. *342*, 309–325.

Cai, X. (2012). Ancient origin of four-domain voltage-gated Na^+ channels predates the divergence of animals and fungi. J. Membr. Biol. *245*, 117–123.

Capella-Gutiérrez, S., Silla-Martínez, J.M., and Gabaldón, T. (2009). trimAl: a tool for automated alignment trimming in large-scale phylogenetic analyses. Bioinformatics *25*, 1972–1973.

Catterall, W.A. (2000). From ionic currents to molecular mechanisms: the structure and function of voltage-gated sodium channels. Neuron *26*, 13–25.

Cestèle, S., and Catterall, W.A. (2000). Molecular mechanisms of neurotoxin action on voltage-gated sodium channels. Biochimie *82*, 883–892.

Chapman, J.A., Kirkness, E.F., Simakov, O., Hampson, S.E., Mitros, T., Weinmaier, T., Rattei, T., Balasubramanian, P.G., Borman, J., Busam, D., et al. (2010). The dynamic genome of *Hydra*. Nature *464*, 592–596.

Cui, Y.J., Yu, L.L., Xu, H.J., Dong, K., and Zhang, C.X. (2012). Molecular characterization of DSC1 orthologs in invertebrate species. Insect Biochem. Mol. Biol. *42*, 353–359.

Derelle, R., and Lang, B.F. (2012). Rooting the eukaryotic tree with mitochondrial and bacterial proteins. Mol. Biol. Evol. *29*, 1277–1289.

Edgar, R.C. (2004). MUSCLE: a multiple sequence alignment method with reduced time and space complexity. BMC Bioinformatics *5*, 113.

Genikhovich, G., and Technau, U. (2009). *In situ* hybridization of starlet sea anemone (*Nematostella vectensis*) embryos, larvae, and polyps. Cold Spring Harb. Protoc. *2009*(9), pdb.prot5282.

Goldin, A.L. (2002). Evolution of voltage-gated $Na(^+)$ channels. J. Exp. Biol. *205*, 575–584.

Guindon, S., Dufayard, J.F., Lefort, V., Anisimova, M., Hordijk, W., and Gascuel, O. (2010). New algorithms and methods to estimate maximum-likelihood phylogenies: assessing the performance of PhyML 3.0. Syst. Biol. *59*, 307–321.

Heinemann, S.H., Terlau, H., Stühmer, W., Imoto, K., and Numa, S. (1992). Calcium channel characteristics conferred on the sodium channel by single mutations. Nature *356*, 441–443.

Hille, B. (2001). Ion Channels of Excitable Membranes, Third Edition (Sunderland, MA: Sinauer Associates Inc.).

Jegla, T.J., Zmasek, C.M., Batalov, S., and Nayak, S.K. (2009). Evolution of the human ion channel set. Comb. Chem. High Throughput Screen. *12*, 2–23.

Liebeskind, B.J., Hillis, D.M., and Zakon, H.H. (2011). Evolution of sodium channels predates the origin of nervous systems in animals. Proc. Natl. Acad. Sci. USA *108*, 9154–9159.

Marlow, H.Q., Srivastava, M., Matus, D.Q., Rokhsar, D., and Martindale, M.Q. (2009). Anatomy and development of the nervous system of *Nematostella vectensis*, an anthozoan cnidarian. Dev. Neurobiol. *69*, 235–254.

Meech, R.W., and Mackie, G.O. (2007). Evolution of excitability in lower metazoans, G. North and J. Greenspann, eds. (New York: Cold Spring Harbor Laboratory Press), pp. 581–615.

Nagahora, H., Okada, T., Yahagi, N., Chong, J.A., Mandel, G., and Okamura, Y. (2000). Diversity of voltage-gated sodium channels in the ascidian larval nervous system. Biochem. Biophys. Res. Commun. *275*, 558–564.

Park, E., Hwang, D.S., Lee, J.S., Song, J.I., Seo, T.K., and Won, Y.J. (2012). Estimation of divergence times in cnidarian evolution based on mitochondrial protein-coding genes and the fossil record. Mol. Phylogenet. Evol. *62*, 329–345.

Payandeh, J., Scheuer, T., Zheng, N., and Catterall, W.A. (2011). The crystal structure of a voltage-gated sodium channel. Nature *475*, 353–358.

Putnam, N.H., Srivastava, M., Hellsten, U., Dirks, B., Chapman, J., Salamov, A., Terry, A., Shapiro, H., Lindquist, E., Kapitonov, V.V., et al. (2007). Sea anemone genome reveals ancestral eumetazoan gene repertoire and genomic organization. Science *317*, 86–94.

Reitzel, A.M., and Tarrant, A.M. (2009). Nuclear receptor complement of the cnidarian *Nematostella vectensis*: phylogenetic relationships and developmental expression patterns. BMC Evol. Biol. *9*, 230.

Sato, C., and Matsumoto, G. (1992). Primary structure of squid sodium channel deduced from the complementary DNA sequence. Biochem. Biophys. Res. Commun. *186*, 61–68.

Schlief, T., Schönherr, R., Imoto, K., and Heinemann, S.H. (1996). Pore properties of rat brain II sodium channels mutated in the selectivity filter domain. Eur. Biophys. J. *25*, 75–91.

Shichor, I., Zlotkin, E., Ilan, N., Chikashvili, D., Stuhmer, W., Gordon, D., and Lotan, I. (2002). Domain 2 of *Drosophila* para voltage-gated sodium channel confers insect properties to a rat brain channel. J. Neurosci. *22*, 4364–4371.

Spafford, J., Grigoriev, N., and Spencer, A. (1996). Pharmacological properties of voltage-gated Na^+ currents in motor neurones from a hydrozoan jellyfish *Polyorchis penicillatus*. J. Exp. Biol. *199*, 941–948.

Watanabe, H., Fujisawa, T., and Holstein, T.W. (2009). Cnidarians and the evolutionary origin of the nervous system. Dev. Growth Differ. *51*, 167–183.

Widmark, J., Sundström, G., Ocampo Daza, D., and Larhammar, D. (2011). Differential evolution of voltage-gated sodium channels in tetrapods and teleost fishes. Mol. Biol. Evol. *28*, 859–871.

Zhang, T., Liu, Z., Song, W., Du, Y., and Dong, K. (2011). Molecular characterization and functional expression of the DSC1 channel. Insect Biochem. Mol. Biol. *41*, 451–458.

Zhou, W., Chung, I., Liu, Z., Goldin, A.L., and Dong, K. (2004). A voltage-gated calcium-selective channel encoded by a sodium channel-like gene. Neuron *42*, 101–112.

Supplemental Information

Cell PRESS
Open ACCESS

EXTENDED EXPERIMENTAL PROCEDURES

Composition of Single Ion Solutions Used in the Analysis of Relative Ion Permeability

The K^+ single ion bath solutions used in this study were made of the following salts (in mM): 96 KCl, 5 HEPES, 1 $MgCl_2$, and 0.5 EGTA, or alternatively of 96 KCl, 5 HEPES, and 1.8 EGTA. Both solutions were adjusted to pH 7.5 with KOH. The reversal potential values obtained in both solutions were similar. $MgCl_2$ was included in order to inhibit Ca^{2+}-inactivated chloride currents (Weber et al., 1995) and EGTA was included to chelate residual Ca^{2+}.

The Na^+ single ion bath solutions contained (in mM) 96 NaCl, 5 HEPES, 1 $MgCl_2$, and 0.5 EGTA, or alternatively 96 NaCl, 5 HEPES, and 1.8 EGTA. Both solutions were adjusted to pH 7.5 with NaOH and gave similar reversal potential values.

qPCR

The main parameters of the qPCR analysis followed an established protocol (Reitzel and Tarrant, 2009). In brief, 19-to 21-nt-long primers with a 45%–55% guanine-cytosine content were designed to span one or more introns and produce amplicons of 72–120 bp with minimal predicted secondary structure (m-fold). A standard curve was constructed from serially diluted plasmids containing a larger portion of each transcript, and 18S ribosomal RNA was used as control. Gene expression was assayed in five developmental stages (embryo: 12 hr to 1 day; early larva: 3–5 days; late larva: 5–8 days; juvenile: 9–13 days; adult: months). RNA extraction and cDNA synthesis were conducted as previously described (Reitzel and Tarrant, 2009). qPCR was performed using iQ SYBR Green Supermix (Bio-Rad) in a MyCycler real-time PCR detection system (Bio-Rad). For each gene, standards and experimental samples were run in duplicates (technical replicates of a single plate). PCR products were subjected to melt curve analysis to ensure amplification of only a single product. The number of molecules per microliter for each gene was calculated by comparing the threshold cycle (Ct) from the sample with the standard curve.

SUPPLEMENTAL REFERENCE

Weber, W.-M., Liebold, K.M., Reifarth, F.W., Uhr, U., and Clauss, W. (1995). Influence of extracellular Ca2+ on endogenous Cl- channels in *Xenopus* oocytes. Pflugers Arch. *429*, 820–824.

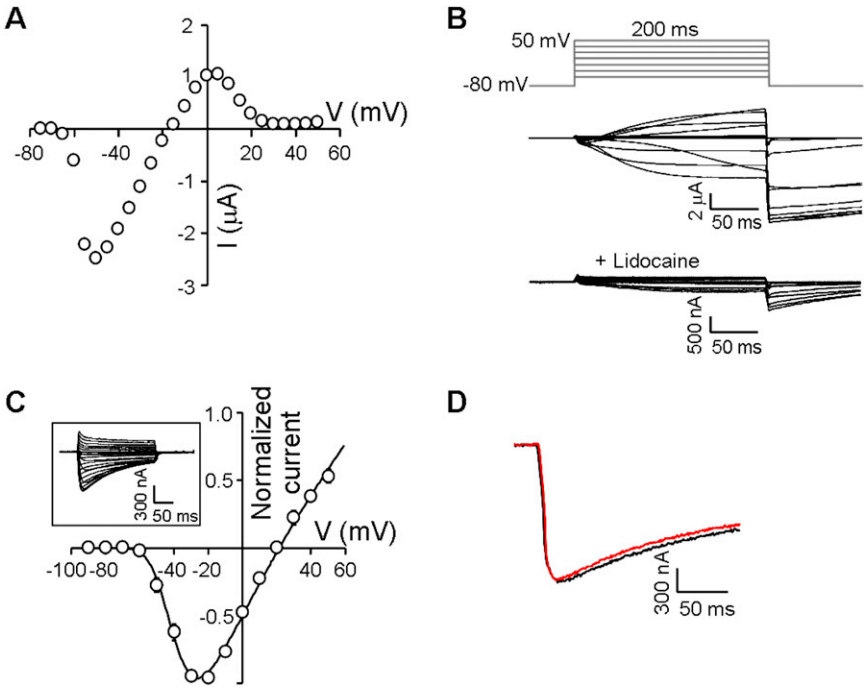

Figure S1. Current Recordings from NvNa$_v$2.1 Expressed in *Xenopus* Oocytes, Related to Figure 1

Oocytes were clamped at −100 or −80 mV holding potential in ND96 bath solution, and currents were elicited by depolarizing pulses from −75 mV to 50 mV for 200 ms.

(A) Current-voltage relations of calcium-activated chloride channels from a representative oocyte, which were activated by Ca^{2+} influx through NvNa$_v$2.1 (E_{rev} = −15.9 mV).

(B) Ca^{2+}-activated Cl^- currents recorded from an oocyte expressing NvNa$_v$2.1. Addition of 5 mM lidocaine reduced the Ca^{2+} inward current through NvNa$_v$2.1, which decreased the chloride currents.

(C) Current-voltage relations of NvNa$_v$2.1 expressed in oocytes injected with BAPTA prior to the measurement (E_{rev} = 21.6 ± 2.2 mV; n = 7). Each point represents mean ± SEM of n cells. Injection of BAPTA to oocytes eliminated the Ca^{2+}-activated Cl^- currents (see inset).

(D) NvNa$_v$2.1 inward current elicited by 200 ms depolarizing pulse to −30 mV with $BaCl_2$ substituting for $CaCl_2$ in the ND96 bath solution. The current was not affected by 100 μM TTX (red).

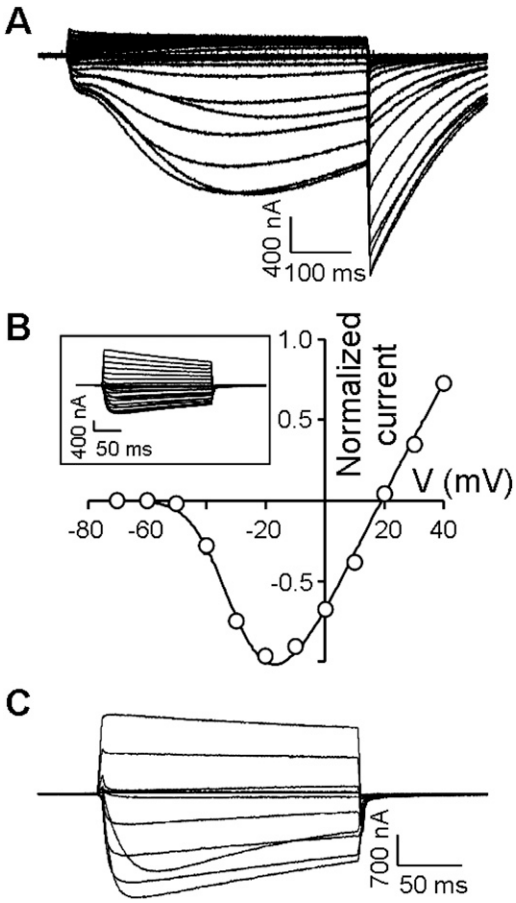

Figure S2. Currents Mediated by Channel Mutants $NvNa_v2.1^{NvNav2.5(p-loops\ DEEA)}$ and $NvNa_v2.1^{NvNav2.5(p-loops\ DEKA)}$ Expressed in Oocytes, Related to Figure 3

(A) Currents elicited by 500 ms depolarizing pulses from −75 to 50 mV mediated by $NvNa_v2.1^{NvNav2.5(p-loops\ DEEA)}$ in ND96 bath solution. Note the large tail currents upon returning to the −80 mV holding potential.

(B) Inward currents elicited by 200 ms depolarizing pulses from −75 to 50 mV mediated by $NvNa_v2.1^{NvNav2.5(p-loops\ DEKA)}$ in ND96 bath solution. Note the absence of tail currents (see inset). The E_{rev} value obtained for the current-voltage relations is 19.1 ± 1.6 (n = 6). Each point represents mean ± SEM of n cells.

(C) Currents elicited by 200 ms depolarizing pulses from −90 to 50 mV mediated by $NvNa_v2.1^{NvNav2.5(p-loops\ DEKA)}$ in K^+ single ion bath solution.

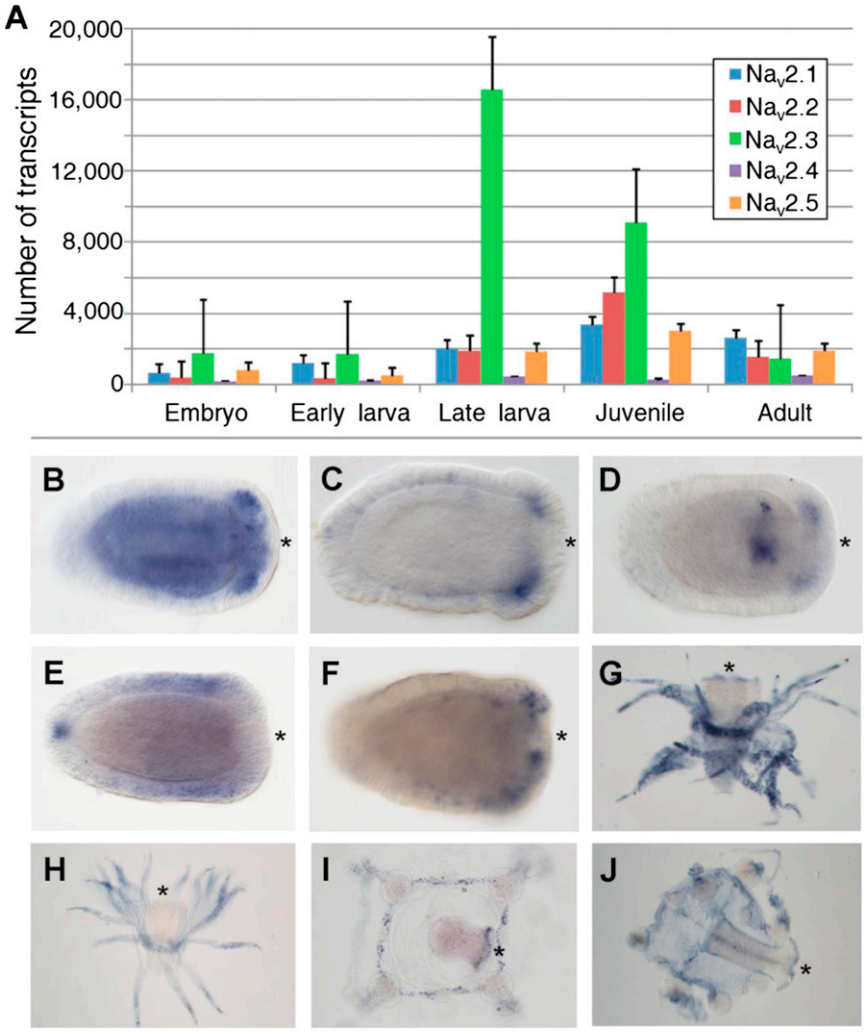

Figure S3. Spatiotemporal Expression of Cnidarian Na$_v$s, Related to Figure 3

(A) Developmental time series of expression for the five Na$_v$2 channel genes from *N. vectensis*. The data were generated from qPCR for five developmental stages. Expression is presented in molecules per μl cDNA. Bars represent mean + SE of n = 3 replicates.

(B–F) In situ hybridization with probes for NvNa$_v$2.1 (B), NvNa$_v$2.2 (C), NvNa$_v$2.3 (D), NvNa$_v$2.4 (E), and NvNa$_v$2.5 (F) revealed the spatial expression pattern of the different channel subtypes in 5-day-old *N. vectensis* larvae. A similar assay on *C. hemisphaerica* revealed the spatial expression patterns of two channel homologs.

(G–J) Probes for ChNa$_v$2.1 (G) and ChNa$_v$2.5 (H) in the gastrozoid developmental stage, and for ChNa$_v$2.1 (I) and ChNa$_v$2.5 (J) in the medusa stage. The oral end is indicated by an asterisk.